LA-UR-97- 2198

CONF-970657--4

Los Alamos National Laboratory is operated by the University of California for the United States Department of Energy under contract W-7405-ENG-36

TITLE: **COMPARISON OF A SPECTRAL TURBULENCE MODEL WITH EXPERIMENTAL DATA OF RAYLEIGH-TAYLOR MIXING**

AUTHOR(S): T(imothy T.) Clark, T-3
F(rancis) H. Harlow, T-3
R(onald W.) Moses, T-3

SUBMITTED TO: *International Workshop on the Physics of Compressible Turbulent Mixing, Marseille, France, June 17–20, 1997*

MASTER

Los Alamos

Los Alamos National Laboratory
Los Alamos, New Mexico 87545

DISCLAIMER

Comparison of a spectral turbulence model with experimental data of Rayleigh-Taylor mixing

T. Clark, F. Harlow and R. Moses
Theoretical Division
Group T-3, Theoretical Hydrodynamics, MSB216
Los Alamos National Laboratory
Los Alamos, New Mexico USA 87545

Abstract: The effects pressure fluctuations present a fundamental difficulty in the formulation of tractable turbulence models. In the regime of incompressible velocity fluctuations,the pressure-velocity correlations are intrinsically nonlocal and can be expressed as an integral over the flow domain wherein the integrand contains two-point velocity correlations. However, engineering transport descriptions of turbulence have traditionally modeled the pressure effects as local, differential functions rather than nonlocal integral relationships. A spectral model proposed by Steinkamp, Clark, and Harlow 1 explicitly incorporates the nonlocal nature of the pressure effects in an inhomogeneous environment. Previous comparisons of model solutions with experimental data showed reasonable agreement at intermediate to high wave numbers 2. However, the lack of detail in previous experimental data has not allowed for a more critical evaluation of the fundamental assumptions incorporated in the model. Recent experiments at Lawrence Livermore National Laboratory (LLNL) by Dimonte et al. provide a richness of detail that is not present in the older data. These data are used to evaluate some of the assumptions of the spectral model of Steinkamp et al., as well as single-point models such as that of Besnard, Harlow, Rauenzahn and Zemach 3. Additionally, simulations of Rayleigh-Taylor instabilities are used to augment the experimental data to give direct insight into the effects of the fluctuating pressure correlations.

1. Introduction

Stochastic, or turbulent, Rayleigh-Taylor mixing introduces significant demands on turbulence closures. Many of the assumptions used in the development of single-point closures for fully developed constant density fluid turbulence may be tenuous at best in the circumstance of developing Rayleigh-Taylor turbulent mixing. For example, the typical approaches to modeling the fluctuating pressure-strain correlations are based on the assumption of nearly homogeneous turbulence. This assumption permits some simplification of the Poisson equation for the pressure-strain terms. However, assumptions of near-homogeneity are clearly questionable at the edge of a Rayleigh-Taylor mixing layer. Another assumption of the standard engineering closures is that the turbulence length-scales can be described by a single length-scale. Such an assumption limits a model's ability to distinguish differences in the geometric orientations of the correlations. Such assumptions have three compelling justifications. First, the resulting models have a proven history of producing useful predictions in a wide range of circumstances; second, experimental data are generally not available to ascertain the adequacy of these assumptions, and third, incorporation of such effects may introduce unwarranted complexities into the models. Nevertheless, increasing demands for physical fidelity in the stringent regime of Rayleigh-Taylor mixing warrants a detailed examination of the underlying assumptions of

[0]More information - Email: ttc@lanl.gov

the closures. Recent experiments of Rayleigh-Taylor mixing conducted at LLNL 4 provide unprecedented detail regarding the density distributions in the mixing zone. These experiments use a linear electric motor (LEM) to accelerate a fluid test cell and laser-induced florescence in conjunction with a thin laser sheet, or "knife" for illumination. The resulting data provide an ideal opportunity to evaluate assumptions regarding the anisotropy of the length-scales associated with fluctuating density-density correlations. Unfortunately, these experiments do not yet provide information regarding fluid velocities or pressures. To provide information on the nature of the velocities and pressures in the configuration of the experimental apparatus, a series of numerical calculations where performed and analyzed to demonstrate the nature of the turbulence production due to pressure effects.

2. The Spectral Model

The spectral model of Steinkamp, Clark and Harlow 2 represents an attempt to extend a simple spectral flux closure for turbulence to the regime of inhomogeneous turbulence. It is an extension of earlier spectral flux models, e.g., the flux model for constant-density isotropic turbulence of Leith 5, the extension of Leith's model to anisotropic and inhomogeneous turbulence due to Besnard, Harlow, Rauenzahn and Zemach 6 and the extension of the Besnard *et al.* work to homogeneous variable density turbulence by Clark and Spitz 7. A principal motivation of the work of the Los Alamos group was to develop a framework for modeling that is free of the heuristic and frequently *ad hoc* nature of the turbulent kinetic energy dissipation-rate equation (i.e., the ϵ-equation). The model of Steinkamp *et al.* also shares a number of features in common with a one-point closure for variable density turbulence developed by Besnard, Harlow and Rauenzahn 3, such as the the treatment of the mass-weighted-averged (Favre) triple velocity correlations. The novel aspect of the model of Steinkamp *et al.* is the treatment of the pressure-production terms in the two-point Reynolds-stress equations as a nonlocal, or integral, term. The motivation for this extension is the simple observation that the movement of fluid at the high/low-density interface of a Rayleigh-Taylor instability is communicated to the fluid at points away from the interface via the pressure acting in conjunction with the incompressibility constraint. The actual derivation of the spectral model of Steinkamp *et al.* is described in detail in 8 as well as 1. The variables are those established by Clark and Spitz 7, including the two-point turbulence Reynolds stress,

$$R_{ij}\left(\mathbf{x}_1,\mathbf{x}_2,t\right) = \overline{\frac{1}{2}\left[\rho\left(\mathbf{x}_1,t\right)+\rho\left(\mathbf{x}_2,t\right)\right]u_i''\left(\mathbf{x}_1,t\right)u_j''\left(\mathbf{x}_2,t\right)}, \tag{1}$$

the two-point turbulence mass flux,

$$a_i\left(\mathbf{x}_1,\mathbf{x}_2,t\right) = \overline{\rho\left(\mathbf{x}_1,t\right)u_i''\left(\mathbf{x}_1,t\right)v'\left(\mathbf{x}_2,t\right)}, \tag{2}$$

where $v = 1/\rho$ is the specific volume of the fluid, and the two-point fluctuating density-specfic volume correlation,

$$b_i\left(\mathbf{x}_1,\mathbf{x}_2,t\right) = -\overline{\rho'\left(\mathbf{x}_1,t\right)v'\left(\mathbf{x}_2,t\right)}. \tag{3}$$

Following Besnard *et al.*, a change of coordinates is introduced;

$$\mathbf{x} = \frac{1}{2}\left(\mathbf{x}_1+\mathbf{x}_2\right), \quad \mathbf{r} = \left(\mathbf{x}_1-\mathbf{x}_2\right), \tag{4}$$

and the variables are Fourier-transformed with respect to the relative coordinate $\mathbf{r}$. At this point, the variables are complex functions of a 7-dimensional argument $(\mathbf{x},\mathbf{k},t)$. In summary, the angular dependence in $\mathbf{k}$ is removed by averaging over all angles in the $\mathbf{k}$-space, thus making the variables real functions of a three-dimensional physical space coordinate, a Fourier wavenumber (rather than a wavevector) and time. Upon integration over all wavenumbers, the variables reduce to more commonly recognized single-point values such as those described by the single-point model of Besnard *et al.*7. The equation for the evolution of the Reynolds stress is

$$
\begin{aligned}
&\frac{\partial R_{ij}(\mathbf{x},k,t)}{\partial t}+\frac{\partial R_{ij}(\mathbf{x},k,t)\,\tilde{U}_n(\mathbf{x},t)}{\partial x_n} \\
&+R_{in}(\mathbf{x},k,t)\frac{\partial \tilde{U}_j(\mathbf{x},t)}{\partial x_n}+R_{jn}(\mathbf{x},k,t)\frac{\partial \tilde{U}_i(\mathbf{x},t)}{\partial x_n} \\
=&\int_{-\infty}^{+\infty}\left[\left(a_i(z')\frac{\partial \overline{P}(z')}{\partial x_j}\right)+\left(a_j(z')\frac{\partial \overline{P}(z')}{\partial x_i}\right)\right]\left[\frac{\exp\left(-2k\left|z'-z\right|\right)}{\int_{-\infty}^{+\infty}\exp\left(-2k\left|z''-z\right|\right)dz''}\right]dz' \\
&+\frac{\partial}{\partial k}\left\{k^2\sqrt{\frac{kR_{nn}(\mathbf{x},k,t)}{\overline{\rho}(\mathbf{x},t)}}\left[-c_1R_{ij}(\mathbf{x},k,t)+c_2k\frac{\partial R_{ij}(\mathbf{x},k,t)}{\partial k}\right]\right\} \\
&+c_m\int_0^k\sqrt{\frac{kR_{nn}(\mathbf{x},k,t)}{\overline{\rho}(\mathbf{x},t)}}dk\left[\frac{1}{3}R_{nn}(\mathbf{x},k,t)-R_{ij}(\mathbf{x},k,t)\right]+c_d\frac{\partial}{\partial x_n}\left(\nu_t\frac{\partial R_{ij}(\mathbf{x},k,t)}{\partial x_n}\right),
\end{aligned}
\tag{5}
$$

for the turbulence mass flux is,

$$
\begin{aligned}
&\frac{\partial a_i(\mathbf{x},k,t)}{\partial t}+\tilde{U}_n(\mathbf{x},t)\frac{\partial a_i(\mathbf{x},k,t)}{\partial x_n}+\frac{R_{in}(\mathbf{x},k,t)}{\left[\overline{\rho}(\mathbf{x},t)\right]^2}\frac{\partial \overline{\rho}(\mathbf{x},t)}{\partial x_n} \\
=&\frac{b(\mathbf{x},k,t)}{\overline{\rho}(\mathbf{x},t)}\frac{\partial \overline{P}(\mathbf{x},t)}{\partial x_j} \\
&-\left[c_{Rp1}k^2\sqrt{a_n(\mathbf{x},k,t)\,a_n(\mathbf{x},k,t)}+c_{Rp2}k\sqrt{\frac{kR_{nn}(\mathbf{x},k,t)}{\overline{\rho}}}\right]a_i(\mathbf{x},k,t) \\
&+\frac{\partial}{\partial k}\left\{k^2\sqrt{\frac{kR_{nn}(\mathbf{x},k,t)}{\overline{\rho}(\mathbf{x},t)}}\left[-c_1a_i(\mathbf{x},k,t)+c_2k\frac{\partial a_i(\mathbf{x},k,t)}{\partial k}\right]\right\} \\
&+c_d\frac{1}{\overline{\rho}(\mathbf{x},t)}\frac{\partial}{\partial x_n}\left(\overline{\rho}(\mathbf{x},t)\,\nu_t\frac{\partial a_i(\mathbf{x},k,t)}{\partial x_n}\right),
\end{aligned}
\tag{6}
$$

and for the density-specific volume correlation is,

$$
\begin{aligned}
&\frac{\partial b(\mathbf{x},k,t)}{\partial t}=\left(\frac{2\overline{\rho}(\mathbf{x},t)-\rho_1-\rho_2}{\rho_1\rho_2}\right)\frac{\partial \overline{\rho}(\mathbf{x},t)\,a_n(\mathbf{x},k,t)}{\partial x_n} \\
&+c_{fb}\left[\left[\overline{v}(\mathbf{x},t)\right]^2\frac{\partial}{\partial x_n}\left(\frac{\overline{\rho}(\mathbf{x},t)}{\overline{v}(\mathbf{x},t)}\right)\right]\frac{\partial k a_n(\mathbf{x},k,t)}{\partial k} \\
&+\frac{\partial}{\partial k}\left\{k^2\sqrt{\frac{kR_{nn}(\mathbf{x},k,t)}{\overline{\rho}(\mathbf{x},t)}}\left[-c_1b(\mathbf{x},k,t)+c_2k\frac{\partial b(\mathbf{x},k,t)}{\partial k}\right]\right\} \\
&+c_d\frac{\partial}{\partial x_n}\left(\nu_t\frac{\partial b(\mathbf{x},k,t)}{\partial x_n}\right).
\end{aligned}
\tag{7}
$$

In this present effort, we restrict our attention to the loss of angular spectral information caused by reduction of the equations from a wavevector dependence to a wavenumber dependence, and to general features of the nonlocality of the pressure production terms in the Navier-Stokes equations. Attempts at direct model comparisons to the LEM experiments and to numerical simulations failed to produce reasonable results. The cause of this lack of agreement has not been positively identified.

3. Density Correlations in the Rayleigh-Taylor Experiments

The two-point fluctuating density-density correlations computed from a single photograph from an LEM experiment are shown in Figures 1 and 2. The correlations are constructed using an averaging procedure that presumes approximate statistical homogeneity in the plane of the mixing layer (i.e., the $X-Y$ plane). Figure 1 shows the correlations at position Z as a function of a separation ΔZ around position Z. Figure 2 shows the correlations at position Z as a function of a separation ΔX around position Z. In both plots, the dark color implies a strong positive correlation and the light color is a strong negative correlation. The background gray coloration at large and small Z reflects a lack of correlation. The long range correlations in Figure 2 at large ΔX probably represent a lack of a statistically meaningful sample size at that separation distance, and should be ignored. These figures indicate that there is a significant difference in the structure of these correlation functions. The argument for neglecting this orientational dependence of the correlations must then rest on the assumption that there is no significant effect in neglecting this feature. Further research is necessary to understand the physical ramifications of the difference in the length-scales.

4. Nonlocal pressure effects in Rayleigh-Taylor mixing simulations

As part of the effort to interpret the LEM data, a series of computations here undertaken to simulate various aspects of the LEM experiments. The computations were conducted with a three-dimensional Navier-Stokes program that was first-order accurate in time and second-order accurate in space. The dimensions and material properties here taken to approximate those of the LEM. The cell size was $73mm$ x $73mm$ x $88mm$ and the fluids were decane ($\rho = 0.73gm/cm^3$) and saltwater ($\rho = 1.43gm/cm^3$). The acceleration was $1g$ (i.e., much lower than the $70g$ used in the experiment). The computational grid was 88 x 88 x 106. Sixteen individual realizations with "stochastically" perturbed interfaces were performed. The averaging methodology also exploited the inherent symmetries of the square cross-section of the box (the $X-Y$ plane). Figure 3 shows the bouyancy production $2a_z\partial\overline{P}/\partial z$ as well as the nonlocal nature of the pressure-strain production $\overline{p'\left(\partial u_z''/\partial z\right)}$, where a double prime denotes the fluctuation about the mass-weighted average velocity and a single prime denotes a fluctation about volume-weighted average. Note that at the edge of the mixing layer, the direct production due to bouyancy vanishes but the actual pressure-strain correlation is nonzero into the unmixed region.

5. Conclusion

The detailed data regarding density distributions provided by the LEM Rayleigh-Taylor experiments at LLNL have provided new information on the nature of the fluctuating density-density correlations. Further research is still necessary to understand the ramifications of the orientational dependence of these correlations observed in the experiments but neglected in the models. The simulations of Rayleigh-Taylor mixing demonstrated the motivations for incorporating the

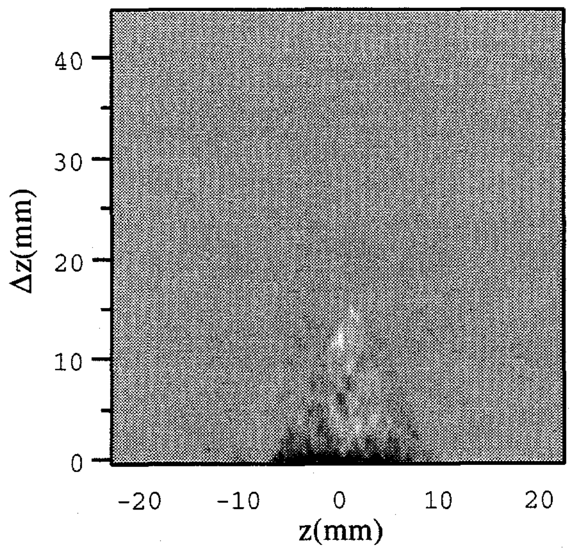

Figure 1. Intensity of two-point fluctuating density correlations $\overline{\rho'(x, z + \Delta z/2)\rho'(x, z - \Delta z/2)}$ averaged over the coordinate x. Data is from a single time from a single experiment. Black is positive, white is negative.

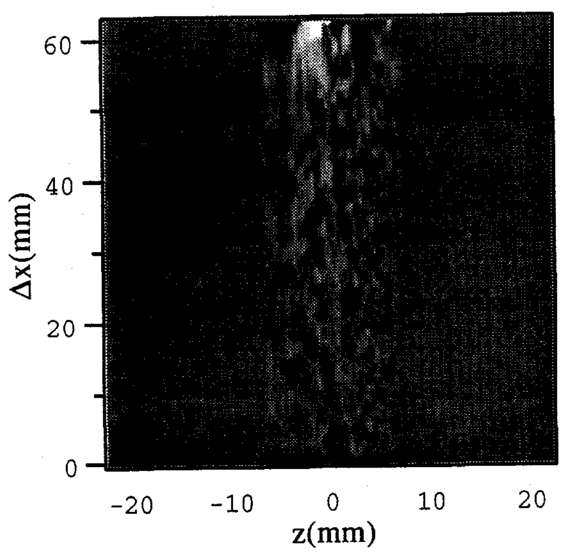

Figure 2. Intensity of two-point fluctuating density correlations $\overline{\rho'(x + \Delta x/2, z)\rho'(x - \Delta x/2, z)}$ averaged over the coordinate x. Data is from a single time from a single experiment. Black is positive, white is negative.

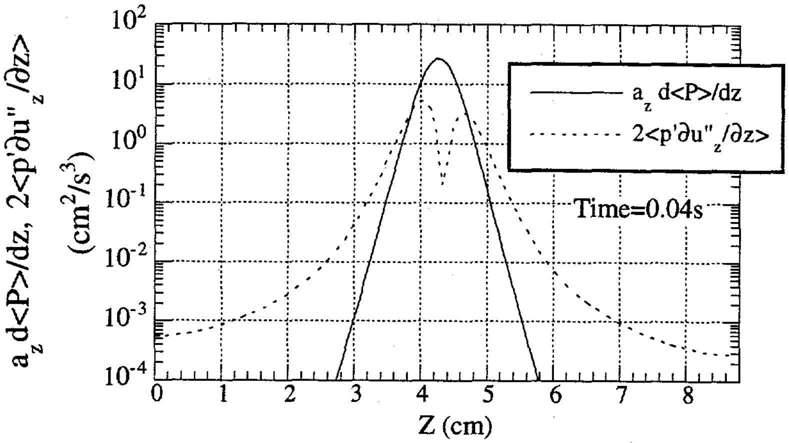

Figure 3. Plot of the pressure production due to turbulent mass flux, and the pressure strain correlation corresponding to the R_{zz} component of the Reynolds stress tensor. Note that the turbulent mass flux, a_z vanishes outside of the actual mixing layer where density fluctuations vanish.

nonlocal pressure production terms in the Steinkamp *et al.* model. However, the relatively low accuracy and resolution of the runs prevents any detailed comparisons of spectra. There exists a significant need for experimental data regarding velocities that is of the same quality as the density distribution data of the LLNL LEM experiment. Additionally, there continues to be a need for robust three-dimensional higher-order computer programs that can handle the sharp discontinuitues that can exist in Rayleigh-Taylor mixing problems.

Acknowledgement. This work is supported by the United States Department of Energy through the Los Alamos National Laboratory LDRD Program.

References

[1] Steinkamp M, Clark T, and Harlow F, Two-Point Description of Two-Fluid Turbulent Mixing. Part 1: Model Formulation, Los Alamos National Laboratory Report LA-UR-96-2038, (1996).

[2] Steinkamp M, Clark T, and Harlow F, Two-Point Description of Two-Fluid Turbulent Mixing. Part 2: Numerical Solutions and Comparisons, Los Alamos National Laboratory Report LA-UR-96-2039, (1996).

[3] Besnard D, Harlow F, Rauenzahn R and Zemach C, Turbulence Transport Equations for Variable-Density Turbulence and Their Relationship to Two-Field Models, Los Alamos National Laboratory Report LA-12303-MS, (1992).

[4] Schneider M, Dimonte G and Remington B, Large and small scale structure in Rayleigh-Taylor mixing, submitted to Phys. Rev. Letters, (1997).

[5] Leith C, Diffusion approximation to inertial energy transfer in isotropic turbulence, Phys. Fluids, 10, 7, 1409-1416, (1967).

[6] Besnard D, Harlow F, Rauenzahn R and Zemach C, Spectral Transport Model of Turbulence, Los Alamos National Laboratory Report LA-11821-MS, (1990).

[7] Clark T, and Spitz P, Two-Point Correlation Equations for Variable Density Turbulence, Los Alamos National Laboratory Report LA-12671-MS, (1995).

[8] Steinkamp M, Spectral Analysis of the turbulent mixing of two fluids, Los Alamos National Laboratory Report LA-13123-T, (1996).